Journal of Applied Polymer Science

Crystallization and Melting Properties of Poly(butylene succinate) Composites with Titanium Dioxide Nanotubes or Hydroxyapatite Nanorods

Jing Zhan,[1] Yangjuan Chen,[1] Gang Tang,[1] Haifeng Pan,[1,2] Qiangjun Zhang,[1] Lei Song,[1] Yuan Hu[1,2]

[1]State Key Laboratory of Fire Science, University of Science and Technology of China, 96 Jinzhai Road, Hefei, Anhui 230026, People's Republic of China

[2]Suzhou Key Laboratory of Urban Public Safety, Suzhou Institute for Advanced Study, University of Science and Technology of China, Suzhou, Jiangsu, People's Republic of China

Correspondence to: Y. Hu (E-mail: yuanhu@ustc.edu.cn)

ABSTRACT: Poly (butylene succinate) (PBS) nanocomposites with titanium dioxide nanotubes (TNTs) or hydroxyapatite nanorods (HAP) were prepared, and the effect of the nano-inorganics on the nonisothermal crystallization and melting properties of PBS were studied in detail by differential scanning calorimeter. The nonisothermal crystallization kinetics of PBS and its nanocomposites were analyzed by the Avrami, Ozawa, and Mo methods. It is found that the presence of TNTs increases the crystallization temperature and rate of PBS composites, but decreases the crystallization activation energy and crystallinity. By comparison, the crystallization rate of the PBS composite is decreased with the addition of HAP. The melting, recrystallization, and remelting mechanism results in the formation of two melting endothermic peaks during the melting process of neat PBS and its nanocomposites. The model proposed by Mo could successfully describe the nonisothermal crystallization process of PBS and its nanocomposites. At a given crystallinity, the $F(t)$ values decrease in the order of PBS/HAP, PBS, and PBS/TNTs. © 2014 Wiley Periodicals, Inc. J. Appl. Polym. Sci. **2014**, *131*, 40335.

KEYWORDS: crystallization; kinetics; differential scanning calorimetry (DSC); biodegradable; composites

Received 16 May 2013; accepted 14 December 2013
DOI: 10.1002/app.40335

INTRODUCTION

Being a rapidly developing biodegradable aliphatic polyester, poly (butylene succinate) (PBS) becomes a research hotspot and holds tremendous applications due to its good mechanical properties, excellent processing capability, and controllable biodegradation rate.[1–3] As a kind of crystalline polymer, the performance of PBS not only depends on its chemical structure and molecular weight, but also is greatly influenced by its crystallization properties, such as crystallization temperature, crystallization rate, crystallinity, and so on.[4,5] The crystallization of PBS can be controlled by adjusting the processing conditions or through modification ways. Products with expected features could be obtained to suit different application requirements.

Inorganic nanoparticles can change the microstructure of the polymer at the molecular scale, and influence the crystallization behaviors and crystalline morphology, thereby improving the thermal stability, mechanical, and processing properties, and so on. Therefore academic and industrial researchers have paid extensive attention to polymer/inorganic nanocomposites. Many inorganic compounds have been introduced into PBS to prepare PBS nanocomposites. It was found that organoclay and silica are good nucleating agents for PBS.[6,7] The addition of functional multiwalled carbon nanotubes (f-MWNT) does not modify the crystal structure of PBS, but enhances the crystallization behavior and thermal stability of PBS composites.[8] The PBS/attapulgite nanocomposite has smaller spherulitic size, higher heat distortion temperature, and Young's modulus.[9]

Recently, titanium dioxide nanotubes (TNTs) and hydroxyapatite nanorods (HAP) have attracted more and more attentions owing to their outstanding physical as well as chemical properties. Titanium dioxide (TiO_2) has been found to have many important applications in areas, such as environmental purification, photocatalyst, gas sensors, and high effect solar cell. Adding TiO_2 into some polymers can obviously improve the thermal and mechanical properties of the polymer composites.[10,11] In Zhou's research, the incorporation of TiO_2 nanofibers into PBS increases the thermal stability, crystallinity, and crystallization rate of the nanocomposites.[11] The research about TNTs grows rapidly, but the investigation of PBS/TNTs composites remains rare. Now hydroxyapatite is mainly used as bone fillers or as a coating in reconstructive surgery. For polymers,

such as HDPE, PLLA, PMMA, hydroxyapatite has also been applied as a reinforcing agent to form bioactive compounds.[12,13] It has been found that the addition of hydroxyapatite can decrease the crystallization rate and onset temperature of PBS, and significantly influence the mechanical properties of PBS composites.[13] It is worth mentioning that there is limited information available about the crystallization kinetics analysis of PBS nanocomposites modified by TNTs or HAP up to now.

In this work, two kinds of inorganic nanocomposites PBS/TNTs and PBS/HAP have been successfully prepared by a solution casting method. Differential scanning calorimeter (DSC) was used to investigate the influences of the additions of TNTs and HAP on the crystallization characteristics and melting behaviors of PBS in detail. The nonisothermal crystallization kinetics was also studied by three different models.

EXPERIMENTAL

Materials

PBS (Mw = 190,000, hydroxyl end-capped) was purchased from Anqing Hexing Chemicals. Powder of titanium dioxide was provided by the Dow Chemical Company. Calcium nitrate, ammonium dihydrogen phosphate, ammonia, sodium hydroxide, hydrochloric acid, and chloroform were all analytical grades and purchased from Sinopharm Chemical Reagent.

Preparation of the Nanoinorganics and Nanocomposites

The preparations of TNTs and HAP by hydrothermal method were described in previous papers.[14,15]

The PBS nanocomposites were fabricated by a solution casting method. About 10 g PBS was first dissolved in 50 mL chloroform, and then 5 wt % of TNTs (HAP) was added into the solution. The mixture was stirred thoroughly, and then ultrasonic treated until a uniformly dispersed suspension was made. The solvent was removed quickly by rotary evaporator, and the resulting viscous liquid was cast on a dish, and further dried in vacuum at 65–70°C for about 12 h. Finally, a sheet of PBS nanocomposites was obtained and kept totally dry in a vacuum drier.

Characterization

Transmission electron microscopy (TEM) image was obtained by a JEOL JEM-2100F transmission electron microscopy with 200 keV accelerated voltage. Scanning electron microscopy (SEM) observations were carried out by high-resolution JEOL JSM-6700 field-emission scanning electron microscopy, and the studied surfaces were first sputter-coated with a thin layer of gold before the measurement. The X-ray diffraction (XRD) measurement was performed by a Japan Rigaku D/Max-γA X-ray diffractometer ($\lambda = 1.54178$ Å), and the samples were thermal compressed into 0.5 mm thick slices. Nonisothermal crystallizations were performed in a Perkin-Elmer Diamond DSC with about 7 mg samples cutting into small granules. The samples were first heated to 140°C, held for 5 min to erase any thermal history, and cooled to 30°C at various cooling rates ranging from 2.5 to 30°C/min. Then, the samples were heated again at a rate of 20°C/min to study the melting behaviors. All the DSC experiments were replicated three times.

RESULTS AND DISCUSSION

Characterization of TNTs, HAP, and PBS Composites

Figure 1 shows the TEM images of TNTs (a) and HAP (b) prepared by hydrothermal methods. It can be observed that the TNTs and HAP crystals have regular morphologies of nanotubes and nanorods with no obvious defects. The diameters of TNTs are around 10 nm and the lengths range from 50 to 300 nm. HAP has a size of 15–30 nm in diameter and 100–200 nm in length.

A homogeneous dispersion of the additive in the polymer matrix can effectively improve the final performances of the composites. To reveal the dispersions of TNTs and HAP in PBS matrix, the fractured surfaces of the samples (frozen well in liquid nitrogen and quickly broken off) were investigated in detail by SEM, and TEM images of the PBS nanocomposites were also shown in Figure 2. It can be seen that TNTs and HAP are dispersed uniformly in the PBS matrix, and no aggregation is observed even in higher magnification images.

It is necessary to study the effect of nano-additives on the crystal structure of PBS. PBS exhibits two kinds of crystal modifications designated as α and β-forms. However, the β-form only exists under strain, and it would transform into the more thermodynamically stable α-form after removal of the strain.[16,17] Figure 3

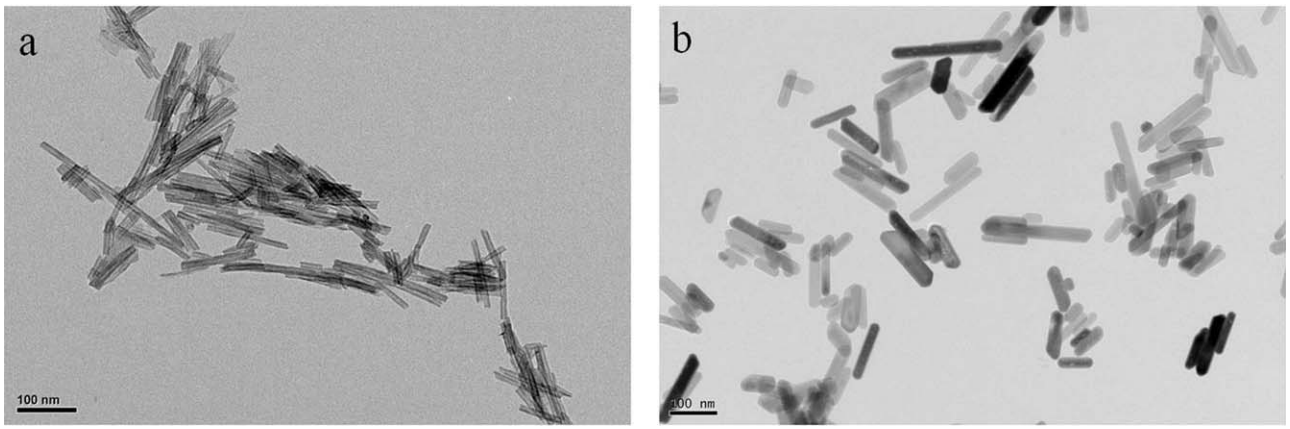

Figure 1. TEM images of TNTs (a) and HAP (b).

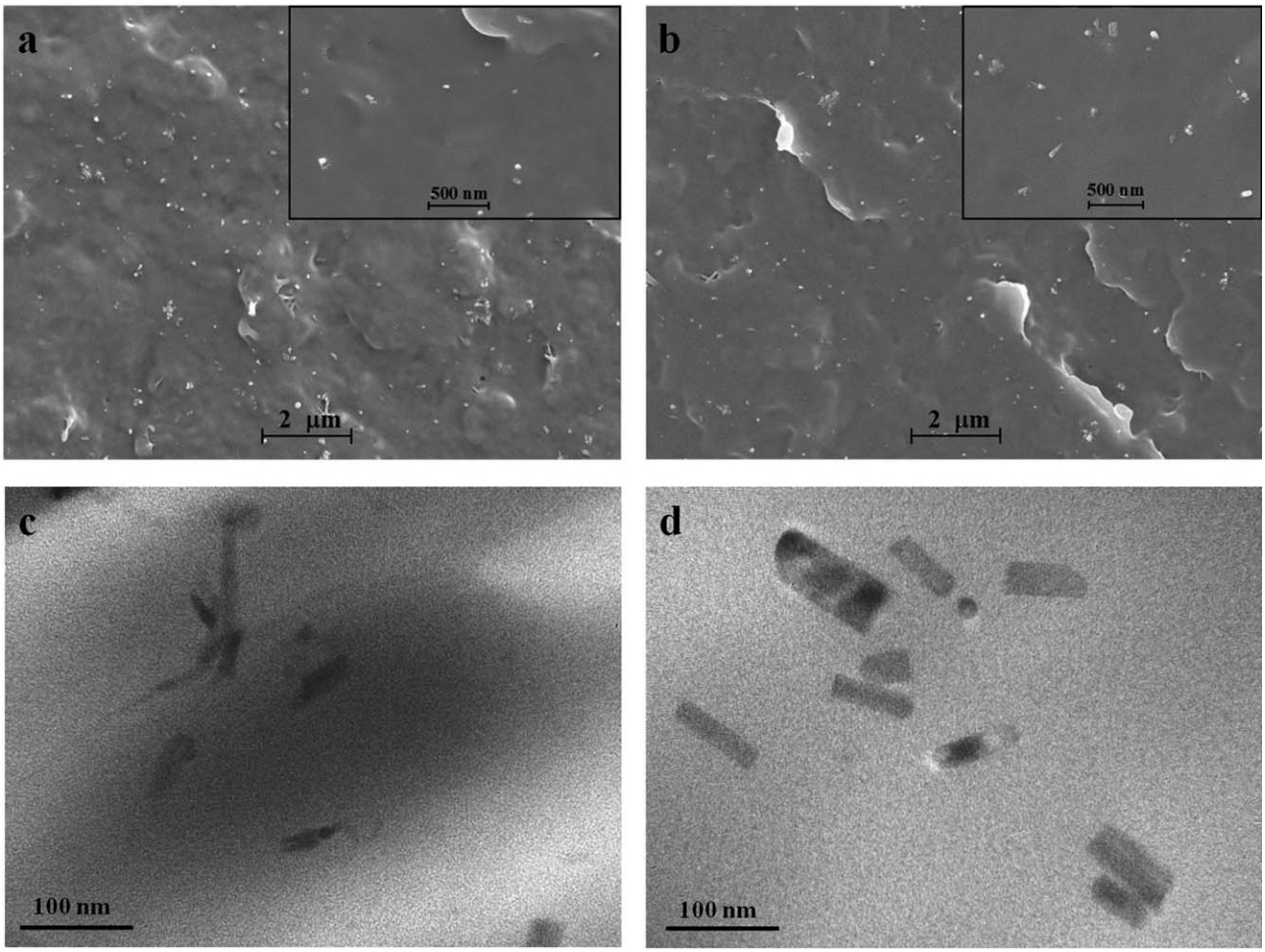

Figure 2. SEM (a, b) and TEM (c, d) images of PBS nanocomposites with TNTs (a, c) and HAP (b, d).

shows the XRD patterns of PBS and its nanocomposites. They exhibit nearly the same diffractions, indicating that the addition of TNTs or HAP does not alter the crystal structure of PBS. The three main peaks located at around 19.7°, 21.9°, and 22.8° are assigned to (020), (021), and (110) planes of the α-form PBS crystal, respectively.[18]

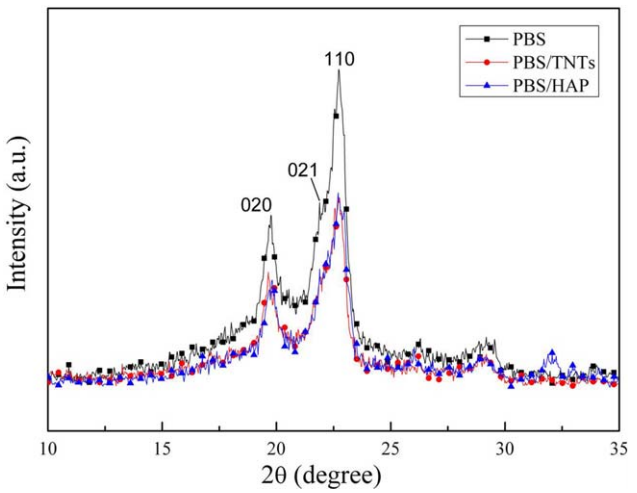

Figure 3. XRD patterns of PBS and its nanocomposites. [Color figure can be viewed in the online issue, which is available at wileyonlinelibrary.com.]

Nonisothermal Crystallization Properties

Most of the practical production and processing of polymer materials are done under nonisothermal conditions, therefore the research of nonisothermal crystallization of polymer is of great technical importance.[19] The DSC curves for nonisothermal crystallization of PBS at different cooling rates (α) are shown in Figure 4. The crystallization exothermic curves shift to lower temperatures and become broader with increasing cooling rate. Some important crystallization parameters of PBS and its nanocomposites, such as the crystallization onset temperature (T_o), crystallization peak temperatures (T_p) and the crystallization enthalpies (ΔH_c), were obtained and listed in Table I. The crystallinity (X) percentages of neat PBS and its nanocomposites were determined by eq. (1):

$$X = \frac{\Delta H_c}{\Delta H_c^0 \times \phi} \times 100\% \quad (1)$$

where the value of crystallization enthalpy of the 100% crystalline PBS (ΔH_c^0) was assumed to be 210 J/g,[20] and ϕ was the content of PBS.

The relative degree of crystallinity (X_T) as a function of temperature at different cooling rates could be calculated as follows:

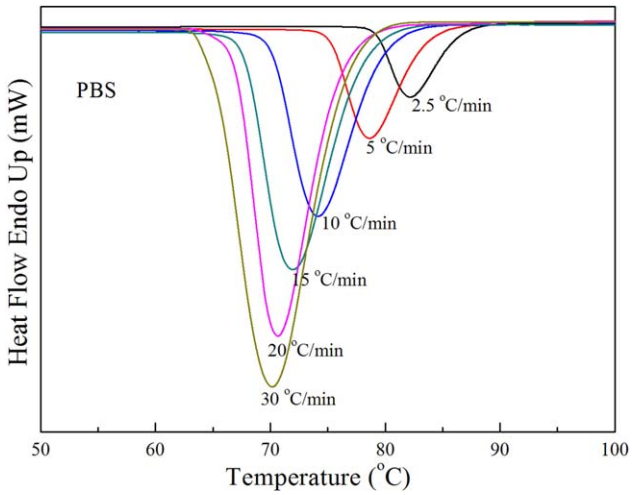

Figure 4. DSC thermograms of nonisothermal crystallization for PBS at various cooling rates. [Color figure can be viewed in the online issue, which is available at wileyonlinelibrary.com.]

$$X_T = \frac{\int_{T_o}^{T} (dH_c/dT)dT}{\int_{T_o}^{T_\infty} (dH_c/dT)dT} \quad (2)$$

where T and T_∞ denote the crystallization temperature at time t and the temperature at the end of the crystallization process, respectively.

Once X_T was obtained, X_t could be carried out by transforming the temperature axis to time axis using the eq. (3):

$$t = (T_o - T)/\alpha \quad (3)$$

The relative degree of crystallinity versus temperature or time for the nonisothermal crystallization of PBS and its nanocomposites at various cooling rates were obtained and the results of PBS are shown in Figure 5. All data of PBS and its nanocomposites give S-type or reversed S-type curves, which are consistent with the nucleation and growth process. From the curves of X_T $(X_t) \sim T(t)$, another important crystallization parameter that can be derived is the half-time of crystallization $(t_{1/2})$, which is defined as the time required to achieve 50% of the final crystallinity of the samples. Usually, the reciprocal of $t_{1/2}$ is proportional to the overall crystallization rate. The $t_{1/2}$ values are also listed in Table I. The crystallization rate becomes faster with the higher cooling rate and smaller $t_{1/2}$.

It can be seen from Table I that under the same cooling rate, T_o and T_p: PBS/TNTs > PBS > PBS/HAP, $t_{1/2}$: PBS/HAP > PBS > PBS/TNTs, and X: PBS > PBS/HAP > PBS/TNTs. These results are consistent with those found from PBS/TiO_2 nanofibers nanocomposites synthesized via *in situ* polymerization and PBS/HAP composites prepared by melt blending method.[11,13]

The influences of TNTs and HAP on the nucleation activity of PBS were studied quantitatively by a method developed by Dobreva and Gotzow.[21,22] For homogeneous nucleation from the melt, the cooling rate can be written as following:

$$\log \alpha = A - \frac{B}{2.303\Delta T_p^2} \quad (4)$$

But for heterogeneous nucleation, the cooling rate is defined as the following:

Table I. The Nonisothermal Crystallization Data of PBS and its Nanocomposites

Sample	α (°C/min)	T_o (°C)	T_p (°C)	ΔH_c (J/g)	X (%)	$t_{1/2}$ (min)
PBS	2.5	88.6	82.1	53.7	25.6	2.9
	5	86.4	78.6	53.3	25.4	1.7
	10	83.5	74.1	53.0	25.2	1.0
	15	82.5	71.9	52.9	25.2	0.7
	20	81.5	70.6	52.3	24.9	0.6
	30	81.2	70.1	51.5	24.5	0.4
PBS/TNTs	2.5	90.4	87.6	47.5	23.8	1.5
	5	88.7	85.3	46.6	23.4	0.8
	10	86.5	82.2	45.9	23.0	0.5
	15	86.3	80.6	45.1	22.6	0.4
	20	85.4	79.2	44.0	22.0	0.3
	30	85.1	78.6	42.2	21.2	0.2
PBS/HAP	2.5	85.5	76.8	51.0	25.6	3.4
	5	83.3	72.5	48.6	24.4	2.0
	10	81.4	67.8	47.9	24.0	1.1
	15	79.6	65.0	46.8	23.4	0.8
	20	78.2	63.6	46.2	23.2	0.7
	30	77.6	63.0	44.5	22.3	0.5

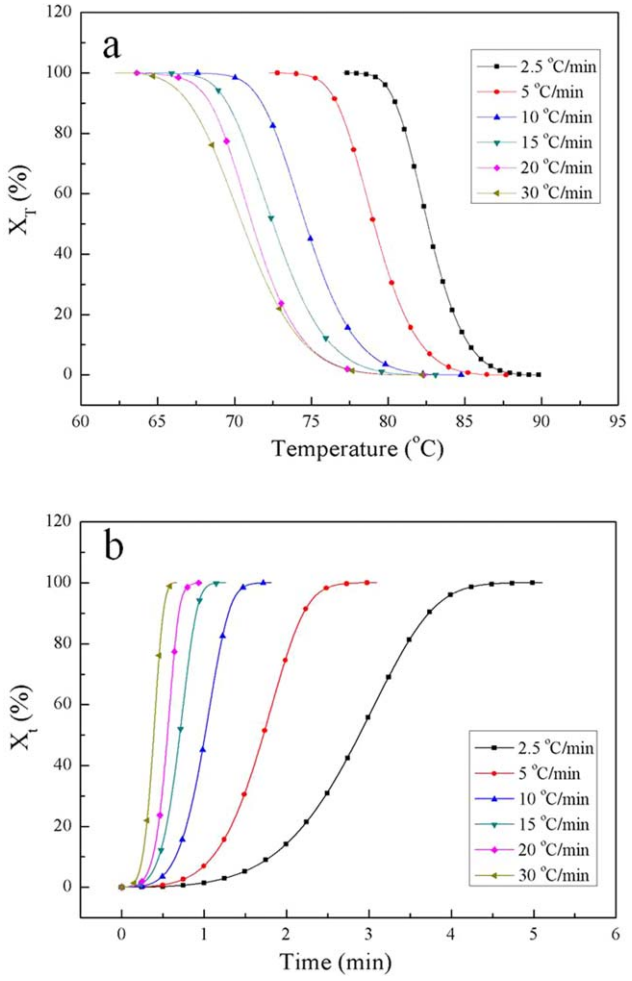

Figure 5. Relative degree of crystallinity versus temperature (a) and time (b) for the nonisothermal crystallization of PBS at various cooling rates. [Color figure can be viewed in the online issue, which is available at wileyonlinelibrary.com.]

$$\log \alpha = A - \frac{B^*}{2.303\Delta T_p^2} \quad (5)$$

where ΔT_p (K) is defined as $T_m - T_p$, and T_m is the melting point temperature corresponding to the end of the melting peak, A, B, and B^* are constants. The ratio of B^*/B is defined as the nucleation activity N. If the foreign substrate is extremely active, the nucleation activity is close to zero, while for the inert particles, the value of N is close to 1.

Figure 6 shows the plots of log α against $1/\Delta T_p^2$, from which the values of B for neat PBS and B^* for its nanocomposites could be obtained from the slopes (k). The nucleation activity of PBS/TNTs and PBS/HAP were estimated to be 0.63 and 1.06. These data indicate that the nucleation activity of PBS is apparently improved by the addition of TNTs, but decreased by HAP.

Usually, the crystallization activation energy (ΔE) indicates the crystallization ability of polymers. The higher the activation energy is, the lower the crystallization ability of the polymer becomes. The effective activation energies for nonisothermal

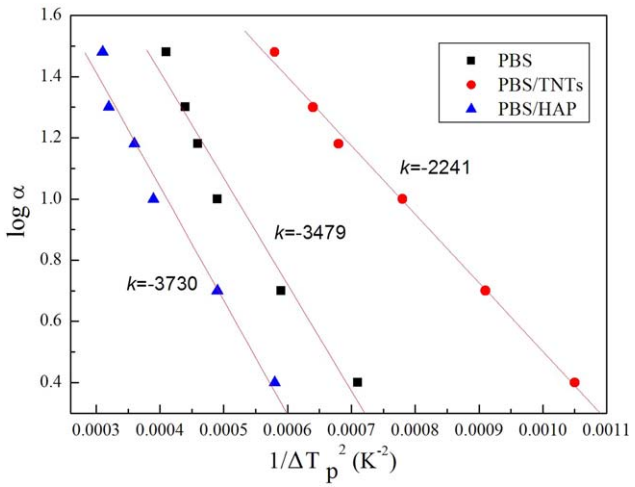

Figure 6. Plots of log α versus $1/\Delta T_p^2$ for the estimation of the nucleation activity. The correlation coefficients of PBS, PBS/TNTs, and PBS/HAP are 0.982, 0.998, 0.988, respectively. [Color figure can be viewed in the online issue, which is available at wileyonlinelibrary.com.]

crystallization of PBS and its nanocomposites were calculated by the method of Friedman:[23]

$$\ln\left(\frac{dX}{dt}\right)_{X,i} = Const - \frac{\Delta E_X}{RT_{X,i}} \quad (6)$$

where dX/dt is the instantaneous crystallization rate as a function of time at a given conversion X, ΔE_X is the effective activation energy at a given conversion X, $T_{X,i}$ is the set of temperatures related to a given conversion X at different cooling rates and the unit of $T_{X,i}$ here is Kelvin (K), and the subscript i refers to every individual cooling rate used. For a constant X, the plot of $\ln(dX/dt)$ versus $1/T_{X,i}$ obtained from curves recorded at several cooling rates, should be a straight line, and the slope of the line is equal to $-\Delta E_X/R$. Thus the effective activation energies as a function of the relative degree of crystallinity were plotted in Figure 7.

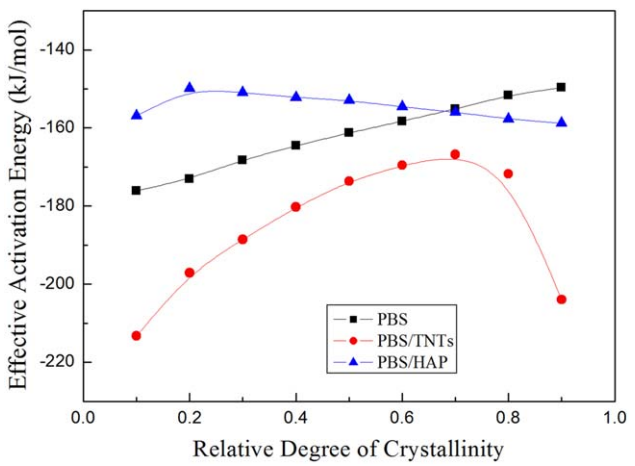

Figure 7. Effective activation energy as a function of the relative degree of crystallinity obtained from the Friedman's method for PBS and its nanocomposites. [Color figure can be viewed in the online issue, which is available at wileyonlinelibrary.com.]

It is found that the effective activation energies of PBS and its composites do not have the same value for all the area of crystallization conversion. The PBS/TNTs nanocomposite always presents lower ΔE values as compared to neat PBS, indicating that the presence of TNTs increases the crystallization ability of PBS. However, the ΔE value of PBS/HAP nanocomposite is higher than that of PBS at the lower relative crystallinity. In addition, the effective activation energies of PBS/TNTs and PBS/HAP have the maximum values at the relative crystallization of 0.7 and 0.2, respectively, corresponding to the lowest crystallization ability of the nanocomposites.

The dependence of the effective activation energies on the relative degree of crystallinity is an indication of at least two different crystallization mechanisms with different activation energies, which are taking place at different degrees of crystallization conversion. According to the secondary nucleation theory which has been formulated from Hoffman and Lauritzen, the overall crystallization rate can be controlled by nucleation and transport of the macromolecules in the melt state.[24] Therefore, it can be deduced that the presence of TNTs decrease the nucleation activation energy of PBS composites as a nucleating agent, and HAP mainly influences the transport of the PBS macromolecules.

For PBS/TNTs nanocomposite, TNTs acts as embryonic crystals or nuclei for the heterogeneous nucleation of polymer chains to accelerate the crystallization of PBS. Hence, the crystallization temperature and rate of PBS/TNTs are higher than that of pure PBS, and its crystallization activation energy gets lower. However the presence of tubular TNTs also plays a role of a constraint on the polymer chains' mobility, especially when they have good interactions with polymer chains, and this result in a decrease of the crystallinity.

The carbon nanotube (CN) has similar structure with TNTs, and its effect on the crystallization property of PBS has been widely studied.[5,25,26] The existing research results show that the incorporation of CN can obviously increase the crystallization temperature of PBS composite, which is similar to the effect of TNTs. With the addition of 3–5 wt % TNTs or CN, the T_p of the obtained PBS nanocomposite can raise about 10 °C. But being different to the complex effect of TNTs, adding CN can also increase the crystalline of PBS nanocomposite.

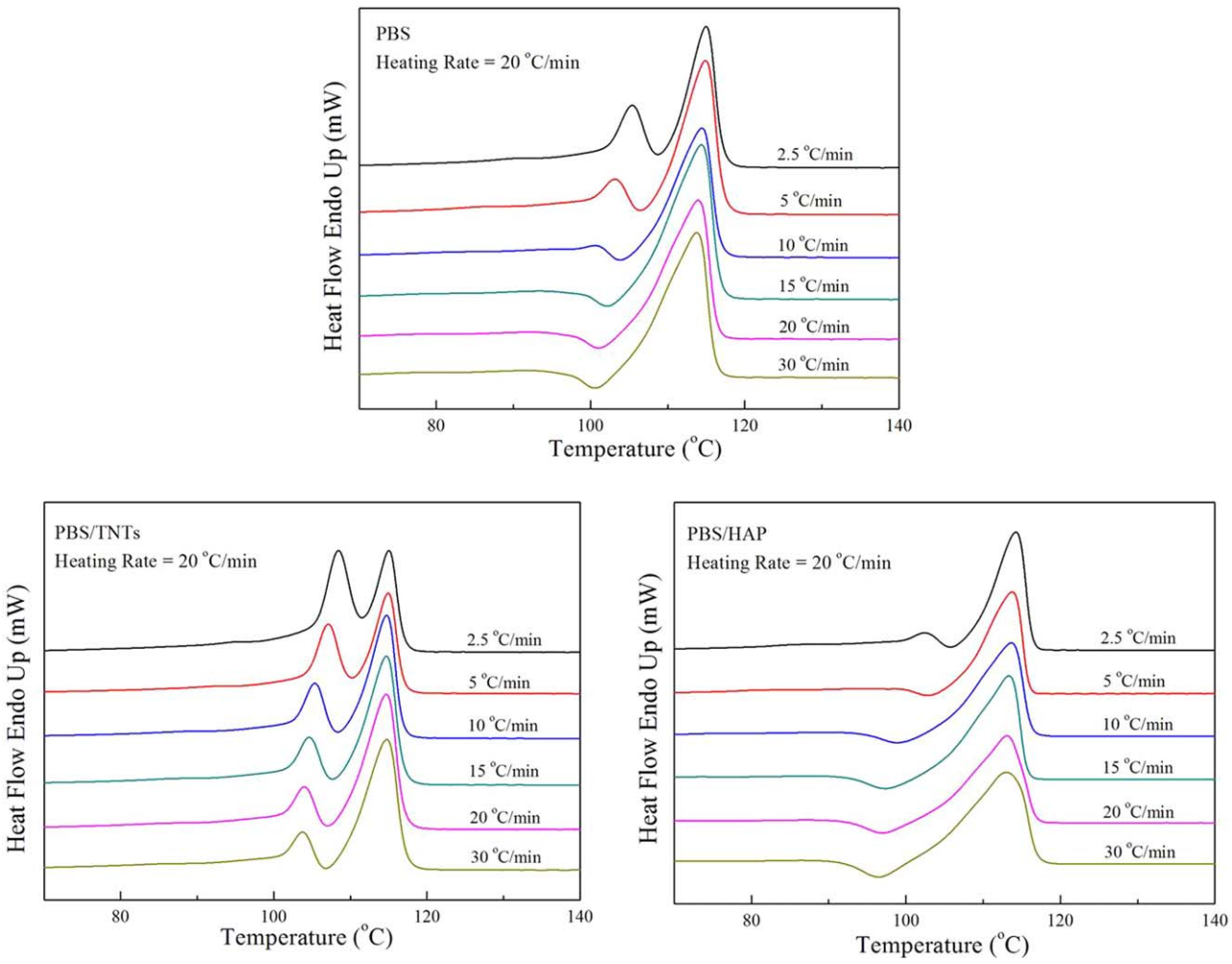

Figure 8. Melting behaviors of PBS and its nanocomposites. [Color figure can be viewed in the online issue, which is available at wileyonlinelibrary.com.]

The hydroxyl groups on the surface of TNTs are unstable and can be dehydrated during the heating process in DSC tests. However, the hydroxyls on the backbone of HAP have extremely high thermal stability.[15] So it is deduced that there is a strong hydrogen bonding effect between HAP and PBS, which could reduce the transport of the PBS macromolecules. Thus, the crystallization temperature and rate of PBS/HAP are lower than that of pure PBS. But on the other hand, the hydrogen bonding interaction between HAP and PBS is good for the crystal growth process and the formation of large crystals.[13]

Melting Behaviors

Subsequent melting behaviors of PBS and its nanocomposites crystallized nonisothermally at various cooling rates were studied by DSC at a heating rate of 20°C/min (Figure 8). Two melting endothermic peaks, denoted as T_{m1} and T_{m2} from low to high temperatures, are observed from the DSC curves for PBS and its nanocomposites. The possibility that the double melting peaks are caused by different crystal structures can be ruled out from the analysis of XRD results. Here the double melting behavior of PBS and its nanocomposites can be ascribed to melting, recrystallization and remelting mechanism with reference to the related literatures.[27,28] During the melting process, some of the polymer chains would gradually dissociate to disordered state with good mobility from the regularly arranged folding state. And then the random chains could be recrystallized using small crystals (orderly arranged bundles of polymer chains that have not been melted) existed in the system as nuclei. Thus, the double melting peaks are emerged. T_{m1} corresponds to the melting of the crystals formed during the nonisothermal melt crystallization, while T_{m2} corresponds to the melting of the crystals formed through melting and recrystallization during DSC heating scans. With increasing cooling rate, T_{m1} shifts to lower temperature, while T_{m2} is almost unchanged. Obviously, the ratio of the intensity of T_{m1} to that of T_{m2} increases with decreasing cooling rate, because the lower the cooling rate becomes during the melt crystallization, the more perfect the crystals (with higher stability) form. Due to the higher crystallization temperature of PBS/TNTs, more stable crystals are produced, thus its first low temperature melting peak is more pronounced.

Nonisothermal Crystallization Kinetics

To further understand the development of crystallization during the nonisothermal crystallization process, the Avrami, Ozawa, and Mo (a combination of the Avrami and Ozawa methods)

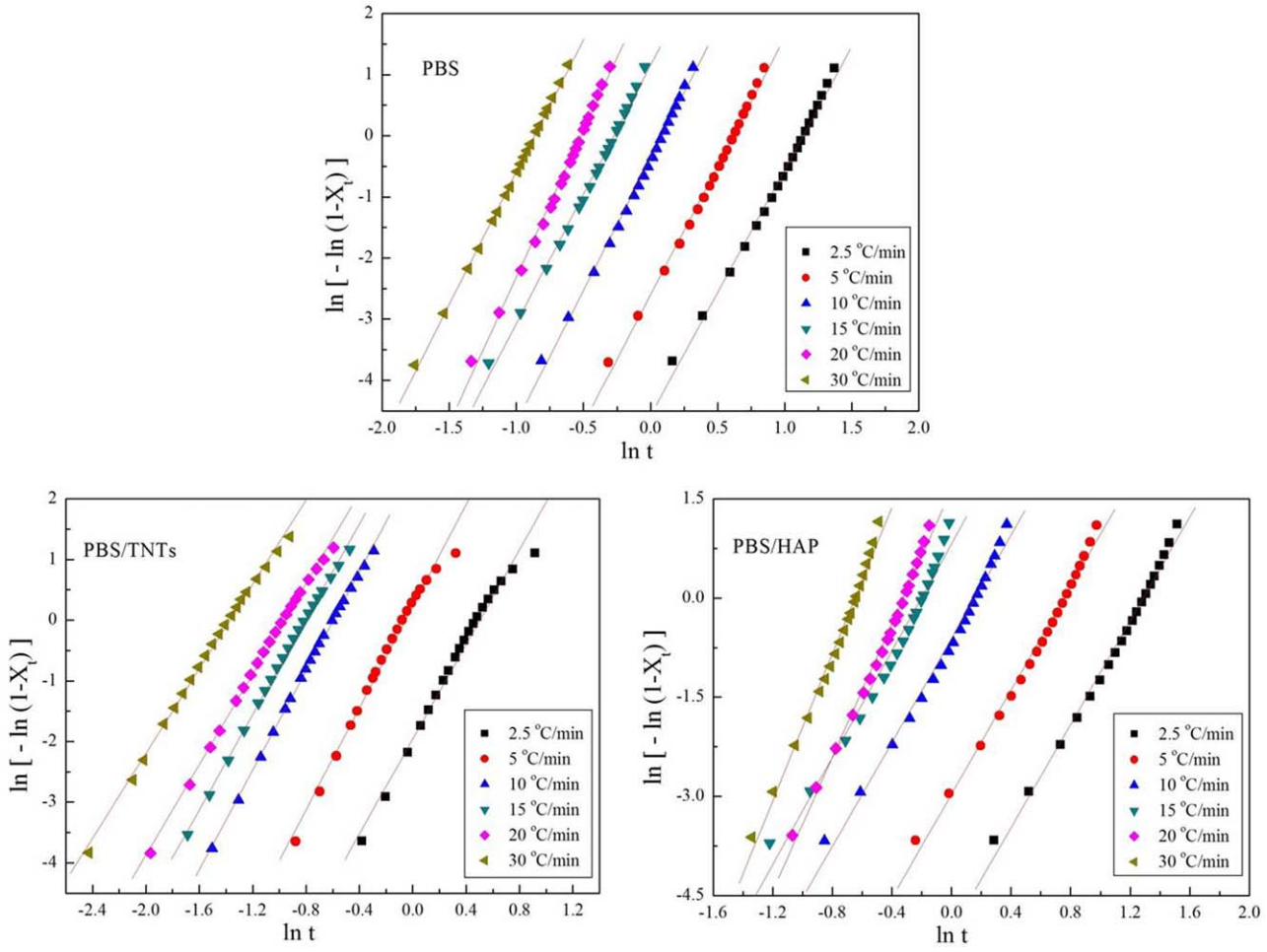

Figure 9. Avrami plots of $\ln[-\ln(1-X_t)]$ versus $\ln t$ for the nonisothermal crystallization of PBS, PBS/TNTs, and PBS/HAP. [Color figure can be viewed in the online issue, which is available at wileyonlinelibrary.com.]

models were applied to analyze the nonisothermal crystallization kinetics of neat PBS and its nanocomposites.[29]

Avrami Method. The well-known Avrami equation is usually applied to analyze the isothermal crystallization kinetics of polymers. It assumes that the relative degree of crystallinity X_t develops as a function of crystallization time t as follows:[30,31]

$$1-X_t=\exp(-kt^n) \quad \text{i.e.,} \quad \ln[-\ln(1-X_t)]=n\ln t+\ln k \tag{7}$$

where X_t is the relative degree of crystallinity at time t, k is the crystallization rate constant, and n is the Avrami exponent depending on the nature of nucleation and growth geometry of the crystals.

Figure 9 is the Avrami plots of $\ln[-\ln(1-X_t)]$ versus $\ln t$ for the nonisothermal crystallization of PBS, PBS/TNTs, and PBS/HAP. It can be found that the linear fitting result of pure PBS is good. But there are some linear deviations for PBS/TNTs and PBS/HAP in the later period of crystallization. This might be caused by the colliding of the spherulites or by a further perfectionism of the crystals.

Taking into account that temperature is a function of time during nonisothermal crystallization, some other methods have been developed on the basis of Avrami equation for the theoretical treatment of nonisothermal crystallization kinetics, such as Ozawa method and Mo method.

Ozawa Method. According to Ozawa theory,[32] the nonisothermal crystallization process is the result of an infinite number of small isothermal crystallization steps, and the degree of conversion at temperature T, X_T can be calculated as:

$$1-X_T=\exp(-K_T/\alpha^m) \quad \text{i.e.,} \quad \ln[-\ln(1-X_T)]=\ln K_T-m\ln\alpha \tag{8}$$

where m is the Ozawa exponent that similar to Avrami exponent, and K_T is the crystallization rate constant, i.e., related to temperature. Figure 10 shows the nonisothermal crystallization kinetics of PBS and its nanocomposites analyzed with Ozawa method. Data analysis was carried out from plots of $\ln[-\ln(1-X_T)]$ versus $\ln\alpha$ within the crystallization temperature range of 78–81°C for neat PBS, 81–84°C for PBS/TNTs, and 72–75°C for PBS/HAP. The nonlinear curves indicate that the Ozawa method is not fitting for describing the nonisothermal crystallization of PBS and its nanocomposites.

Mo Method. Mo's model is a combination of Avrami and Ozawa equations.[33] The importance of this method is that it correlates cooling rate α to the crystallization time t and the morphology for a given degree of crystallinity as follows:

$$\ln\alpha=\ln F(t)-a\ln t \tag{9}$$

where $F(t)=(K_T/k)^{1/m}$ refers to the value of the cooling rate at which the system should have a certain degree of crystallinity at a unit crystallization time, and a is the ratio of the Avrami exponent (n) to Ozawa exponent (m), i.e., $a=n/m$.

As shown in Figure 11, at a given degree of crystallinity, the plot of $\ln\alpha$ against $\ln t$ forms a straight line with an intercept of $\ln F(t)$ and a slope of $(-a)$. The $F(t)$ and a values obtained from the straight lines are listed in Table II. All the correlation coefficients for the best-fit lines of PBS, PBS/TNTs, and PBS/HAP are higher than 0.998, meaning that Mo equation is fully

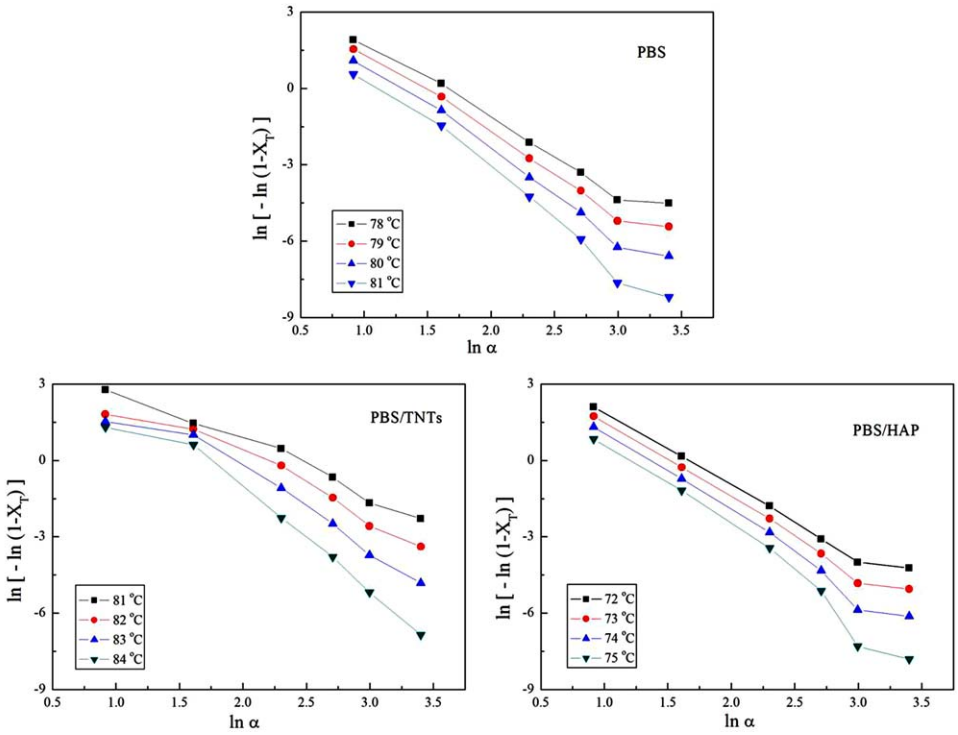

Figure 10. Ozawa plots of $\ln[-\ln(1-X_T)]$ versus $\ln\alpha$ for the nonisothermal crystallization of PBS, PBS/TNTs, and PBS/HAP. [Color figure can be viewed in the online issue, which is available at wileyonlinelibrary.com.]

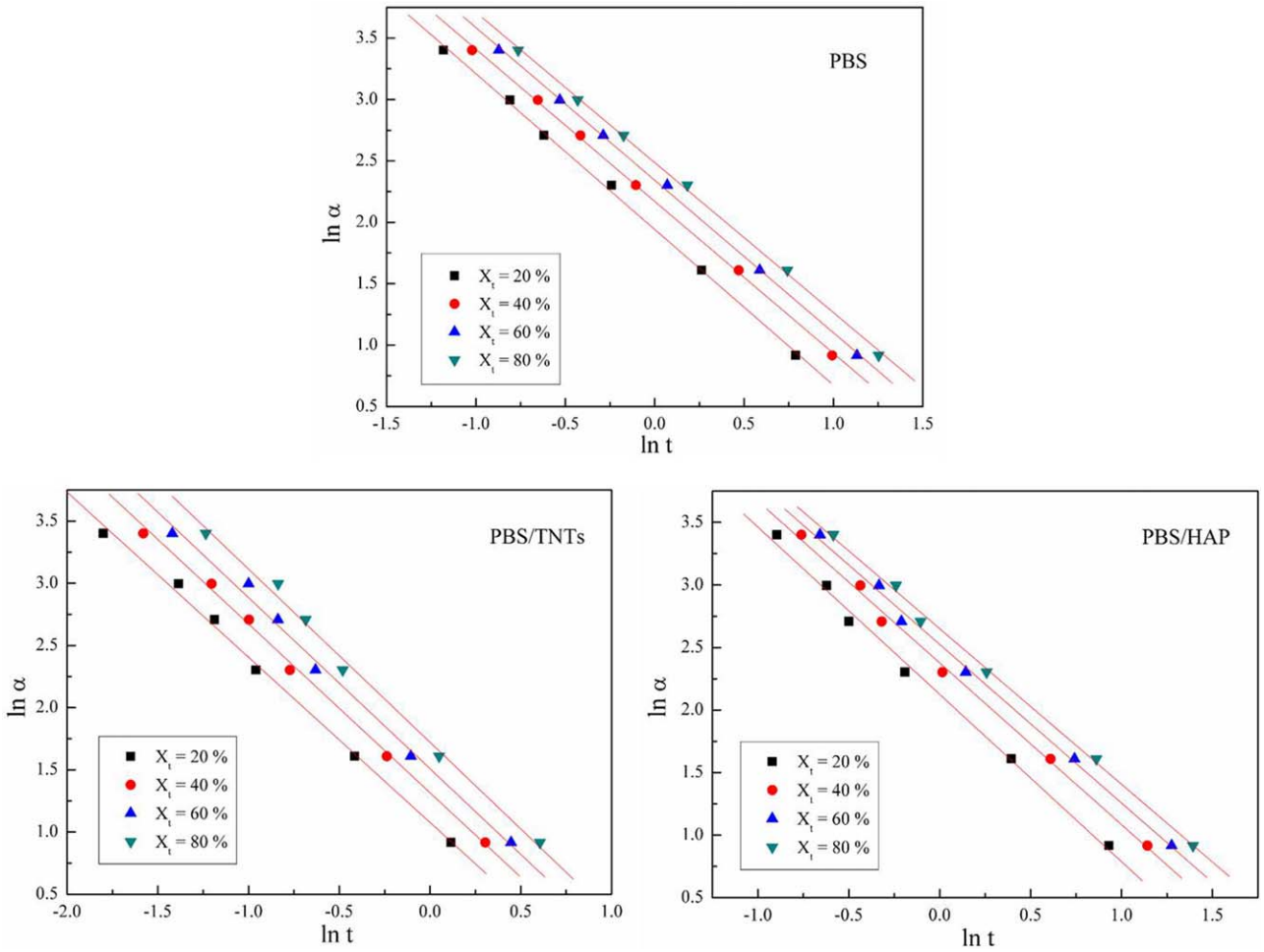

Figure 11. lnα versus ln*t* from Mo equation for the nonisothermal crystallization of PBS, PBS/TNTs, and PBS/HAP. [Color figure can be viewed in the online issue, which is available at wileyonlinelibrary.com.]

fit for describing the nonisothermal crystallization kinetics of PBS and its nanocomposites.

The values of *a* for PBS/TNTs are higher than that of PBS and PBS/HAP, indicating that the addition of TNTs changed the nucleation mechanism of PBS. The values of *a* are almost independent of the crystallinity, and this result means there is a linear relationship between *n* and *m*. The *F*(*t*) values of PBS, PBS/TNTs, and PBS/HAP are all increased with the increasing degree

Table II. Values of *F*(*t*) and a Versus Degree of Crystallinity Based on Mo's Treatment for PBS and its Nanocomposites

Sample	X_t (%)	*F*(*t*)	*a*
PBS	20	6.96	1.27
	40	8.76	1.24
	60	10.38	1.24
	80	12.06	1.22
PBS/TNTs	20	2.92	1.33
	40	3.71	1.35
	60	4.53	1.38
	80	5.58	1.39
PBS/HAP	20	8.41	1.34
	40	10.80	1.29
	60	12.43	1.27
	80	14.15	1.24

of crystallinity. $F(t)$ values can represent the crystallization rate, and the bigger the $F(t)$ value is, the lower the crystallization rate is. At a given crystallinity, $F(t)$: PBS/TNTs < PBS < PBS/HAP, indicating that the crystallization rates: PBS/TNTs > PBS > PBS/HAP. This result confirms that TNTs is a good nucleating agent for PBS, and the presence of HAP inhibits the crystallization process of PBS due to the hydrogen bonding interaction. In summary, the Mo equation can successfully analyze the nonisothermal crystallization kinetics of PBS and its nanocomposites prepared in this work.

CONCLUSIONS

In this work, PBS nanocomposites with TNTs and HAP were prepared by a solution casting method. Influences of TNTs and HAP on the nonisothermal crystallization and melting properties of PBS were studied in detail by DSC. It is found that TNTs play a role of heterogeneous nucleating agent, increasing the crystallization temperature and rate of PBS composite, and decreasing its crystallization activation energy. By comparison, there exists a strong hydrogen bonding interaction between HAP and PBS, which can reduce the transport of the PBS macromolecules. Therefore, the crystallization rate of PBS/HAP composite is lower than that of pure PBS.

Two endothermic peaks appear in the DSC curves during the melting process of PBS and its nanocomposites, and this phenomenon could be ascribed to the melting, recrystallization, and remelting mechanism. The trend of the formation of double melting peaks is PBS/TNTs > PBS > PBS/HAP.

It is found that the Mo method as a combination of Avrami and Ozawa methods can successfully analyze the nonisothermal crystallization kinetics of PBS and its nanocomposites. At a given crystallinity, the $F(t)$ values decrease in the order of PBS/TNTs < PBS < PBS/HAP.

ACKNOWLEDGMENTS

The work was financially supported by the National Basic Research Program of China (973 Program) (2012CB719701), the National Natural Science Foundation of China (No.51303165), and the joint fund of NSFC and CAAC (No. 61079015).

REFERENCES

1. Han, Y.; Sung, R.; Kim, *J. Macromol. Res.* **2002**, *10*,108.
2. Fujimaki, T. *Polym. Degrad. Stabil.* **1998**, *59*, 209.
3. Gan, Z.; Abe, H.; Kurokawa, H.; Doi, Y. *Biomacromolecules* **2001**, *2*, 605.
4. Maiti, P.; Nam, P. H.; Okamoto, M.; Hasegawa, N.; Usuki, A. *Macromolecules* **2002**, *35*, 2042.
5. Wang, G. L.; Guo, B. H.; Xu, J.; Li, R. *J. Appl. Polym. Sci.* **2011**, *121*, 59.
6. Chen, G. X.; Kim, E. S.; Yoon, J. S. *J. Appl. Polym. Sci.* **2005**, *98*, 1727.
7. Bian, J. J.; Han, L. J.; Wang, X. M.; Wen X.; Han, C. Y.; Wang, S. S.; Dong, L. S. *J. Appl. Polym. Sci.* **2010**, *116*, 912.
8. Song, L.; Qiu, Z. B. *Polym. Degrad. Stabil.* **2009**, *94*, 632.
9. Chen, C. H. *J. Phys. Chem. Solids* **2008**, *69*, 1411.
10. Do, G. H.; Chen, Q.; Che, R. C.; Yuan, Z. R.; Peng, L. M. *Appl. Phys. Lett.* **2011**, *79*, 3702.
11. Zhou, W. D.; Xu, T.; Wang, X. W.; Zhi, E.; Liu, J.; Zhang, W.; Ji, K. H. *J. Appl. Polym. Sci.* **2013**, *127*, 733.
12. Correlo, V. M.; Boesel, L. F.; Bhattacharya, M.; Mano, J. F.; Neves, N. M.; Reis, R. L. *Macromol. Mater. Eng.* **2005**, *290*, 1157.
13. Guo, W. M.; Zhang, Y. H.; Zhang, W. *J. Biomed. Mater. Res. A* **2013**, *101*, 2500.
14. Wu, Y.; Song, L.; Hu, Y. *Polym. Plast. Technol. Eng.* **2012**, *51*, 647.
15. Dong, Y. Y.; Gui, Z.; Jiang, S. H.; Hu, Y.; Zhou, K. Q. *Ind. Eng. Chem. Res.* **2011**, *50*, 10903.
16. Ichikawa, Y.; Kondo, H.; Igarashi, Y.; Noguchi, K.; Okuyama, K.; Washiyama, *J. Polymer* **2000**, *41*, 4719.
17. Ichikawa, Y.; Suzuki, J.; Washiyama, J.; Moteki, Y.; Notguchi, K.; Okuyama, K. *Polymer* **1994**, *35*, 3338.
18. Ihn, K. J.; Yoo, E. S.; Im, S. S. *Macromolecules* **1995**, *28*, 2460.
19. Di Lorenzo, M. L.; Silvestre, C. *Prog. Polym. Sci.* **1999**, *24*, 917.
20. Papageorgiou, G. Z.; Bikiaris, D. N. *Polymer* **2005**, *46*, 12081.
21. Dobreva, A.; Gutzow, I. *J. Non-Cryst Solids* **1993**, *162*, 1–12.
22. Dobreva, A.; Gutzow, I. *J. Non-Cryst Solids* **1993**, *162*, 13–25.
23. Friedman, H. L. *J. Polym. Sci.* **1964**, *C6*, 183.
24. Papageorgiou, D. G.; Papageorgiou, G. Z.; Bikiaris, D. N.; Chrissafis K. *Eur. Polym. J.* **2013**, *49*, 1577.
25. Tan, L. C.; Chen, Y. W.; Zhou, W. H.; Ye, S. W.; Wei, J. C. *Polymer* **2011**, *52*, 3587.
26. Ali, F. B.; Mohan, R. *Polym. Composit.* **2010**, *31*, 1309.
27. Yasuniwa, M.; Satou, T. *J. Polym. Sci. Part B: Pol. Phys.* **2002**, *40*, 2411.
28. Yasuniwa, M.; Tsubakihara, S.; Satou, T.; Iura, K. *J. Polym. Sci. Part B: Pol. Phys.* **2005**, *43*, 2039.
29. Papageorgiou, G. Z.; Achilias, D. S.; Bikiaris, D. N. *Macromol. Chem. Phys.* **2007**, *208*, 1250.
30. Avrami, M. *J. Chem. Phys.* **1939**, *7*, 1103.
31. Jeziorny, A. *Polymer* **1978**, *19*, 1142.
32. Ozawa, T. *Polymer* **1971**, *12*, 150.
33. Liu, T. X.; Mo, Z. S.; Wang, S. G.; Zhang, H. F. *Polym. Eng. Sci.* **1997**, *37*, 568.